GEOPHYSICS. VOL. 76, NO. 5 (SEPTEMBER-OCTOBER 2011); P. WB209–WB216, 11 FIGS.
10.1190/GEO2010-0312.1

Reverse time migration of multiples for subsalt imaging

Yike Liu[1], Xu Chang[1], Degang Jin[2], Ruiqing He[3], Hongchuan Sun[4], and Yingcai Zheng[5]

ABSTRACT

Some hydrocarbon reservoirs are trapped beneath salt bodies, where seismic imaging is greatly challenged due to poor illumination. Multiple reflections have different propagation wave paths from primary reflections and thus can be used to complement the illuminations where primary reflections from beneath the salt are not acquired. Consequently, migration of multiples can sometimes provide better subsalt images compared to conventional migration which uses primary reflections only. In this paper, we propose to modify conventional reverse time migration so that multiples can be used as constructive reflection energy for subsalt imaging. This new approach replaces the impulsive source wavelet with the recorded data containing both primaries and multiples and uses predicted multiples as the input data instead of primary reflections. In the reverse time migration process, multiples recorded on the surface are extrapolated backward in time to each depth level, and the observed data with both primaries and multiples are extrapolated forward in time to the same depth levels, followed by a crosscorrelation imaging condition. A numerical test on the Sigsbee2B data set shows that a wider coverage and a more balanced illumination of the subsurface can be achieved by migration of multiples compared with conventional migration of primary reflections. This example demonstrates that reverse time migration of multiples might be a promising method for complex subsalt imaging.

INTRODUCTION

Geologists have recognized for several decades that some hydrocarbon reservoirs use salt body as the seal rock, whereas geophysicists have found that subsalt imaging meets a great challenge, particularly at the locations where high velocities and structurally varying salt bodies act as sonic lenses that disperse or focus seismic signals. Many recent advances in seismic imaging technology have been in response to these salt-related problems (O'Brien and Gray, 1996, Kessinger and Ramaswamy, 1996, Rosenberg, 2000, Glogovsky et al., 2002, Huang et al., 2009, Liu, F. et al., 2009). Many of the aforementioned approaches have shown improved imaging quality; however, for complicated subsalt areas where primary reflections are unable to illuminate, it remains a challenging issue to obtain satisfactory imaging results.

Multiples are waves that are reflected or scattered more than once at the subsurface interfaces and eventually end up at the seismic receivers. Multiples usually travel with longer wave paths and cover larger areas than primaries in the media. Very often, multiples can penetrate into the earth to illuminate the shadow zones which primaries cannot reach. In addition, multiples usually contain smaller reflection angles than primaries (Berkhout and Verschuur, 2003), and provide the fine structures of the earth. Unlike conventional imaging approaches, which migrate primary reflections only and treat multiples as noise, migration with multiples utilizes multiples as constructive signals for subsurface imaging (Guitton, 2002, Shan, 2003, Muijs et al., 2007, Vasconcelos et al., 2008). In order to migrate multiples, the most straightforward approach is to transform multiples into primaries and then migrate them using conventional migration methods (Verschuur and Berkhout, 2005). The idea of extracting valuable events directly from multiples dates back to the work of Claerbout (1968) on seismic interferometry, which showed how Green's functions (i.e., impulse response of a point source) on the earth's surface could be obtained by auto-correlating traces generated by buried sources. In this case, the summation is applied over buried sources with unknown source locations and excitation times, so the approach was considered as a passive seismic method. That means that the correlation and summation of seismograms leads to virtual events with shorter raypaths and source-receiver geometries closer to the target zone. In this way,

Manuscript received by the Editor 24 September 2010; revised manuscript received 11 March 2011; published online 21 November 2011.
[1]Chinese Academy of Sciences, Institute of Geology and Geophysics, Beijing, CN. E-mail: ykliu@mail.igcas.ac.cn; changxu@mail.igcas.ac.cn.
[2]Sichuan Geophysical Company, CNPC, Chengdu, China. E-mail: degang.jin@gmail.com.
[3]Paulsson Inc., USA, Los Angeles, Calif., USA. E-mail: ruiqing.he@paulsson.com.
[4]University of Utah, currently at ExxonMobil, Houston, Tex., USA. E-mail: hongchuan.sun@exxonmobil.com.
[5]Massachusetts Institute of Technology, Department of Earth, Atmospheric, and Planetary Sciences, Cambridge, Mass., USA. E-mail: yczheng@mit.edu.

the multiples are kinematically transformed to primary reflections with virtual sources on the surface. There have been other efforts in the fields of multiple migration using seismic interferometry (Sheng, 2001, Yu and Schuster, 2002, Schuster et al., 2004, Jiang et al., 2007). He et al. (2007) demonstrated a successful example of 3D wave-equation migration of multiples in VSP (vertical seismic profile) data.

Another solution for migration of multiple is least-squares migration (He and Schuster, 2003, Brown and Guitton, 2005). Cable data recorded at deep ocean bottoms can also be used to image both primary reflections and ghosts against the surface (Reiter et al., 1991). A feedback model and inverse wavefield extrapolation were utilized for multiple migration by transforming multiples into primary reflections (Berkhout and Verschuur, 1994). We extend this methodology to process surface data with standard prestack migration operators, but we do not need to transform multiples into primaries. Kirchhoff, one-way wave-equation and reverse time migration approaches can be used as tools for migration of multiples. Kirchhoff-type imaging methods assume high-frequency approximation to the wave equation and are not accurate enough for imaging geological structures where complex wave phenomena exist. The one-way wave equation method, on the other hand, can provide an efficient and flexible solution to the imaging problem. A more accurate approach, however, is the two-way wave equation based reverse time migration (RTM) method (Whitmore., 1983) which does not have the angle limitation of one-way propagators, and is also capable of imaging complex structures where turning waves and prismatic waves occur. In our approach, a RTM scheme is modified to image multiple reflections to their correct locations in the subsurface. This new approach replaces the impulsive source with the recorded data including both primaries and multiples on the surface, and then replaces the recorded primary reflection data with multiples. Synthetic tests show that the proposed method can effectively image beneath the salt, leading to a promising method for complex subsalt imaging.

METHODOLOGY

We propose to modify a conventional RTM scheme so that it can migrate multiple reflections to their correct locations in the subsurface. This approach replaces the numerical impulsive source with the recorded data including primaries and multiples on the surface, and replaces the recorded primary reflection data with multiples. In the RTM process, multiples recorded on the surface are extrapolated backward in time to each depth level, while primaries and multiples recorded on the surface are extrapolated forward in time to the same depth levels. The imaging condition consists of crosscorrelating the two wavefields at each depth level.

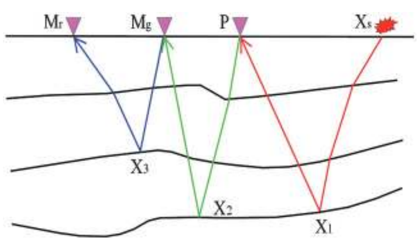

Figure 1. Illustration of RTM of multiples. The first-order multiple recorded at Mg can be backward extrapolated to X2 and cross correlated with the forward extrapolated wavefield of primary reflection recorded at P. The first-order multiple recorded at Mg can also be forward extrapolated to X3 and crosscorrelated with the backward extrapolated wavefield of the second-order multiple recorded at Mr.

Our migration-of-multiple method is divided into two steps. The first step is to obtain multiples using multiple prediction approaches such as Radon transform, predicted deconvolution, and surface-related multiple elimination (SRME) (Verschuur et al., 1992). The second step is to apply reverse time migration for subsalt depth imaging. As a two-way wave-equation based method, RTM is able to handle overhanging structures and strong lateral velocity contrasts.

Reverse time migration of multiples

An explosive source on the surface transmits waves into the earth, and in the frequency domain the media's response to the source can be expressed as

$$D(z_0, z_0) = -X^{\sim} S(z_0, z_0), \qquad (1)$$

where $D(z_0, z_0)$ represents the observed seismic data which normally consists of both primaries and multiples, $X^{\sim}$ is the response matrix of the earth, and $S(z_0, z_0)$ represents the source wavelet. After removing multiples from $D(z_0, z_0)$, we can migrate primary reflections using migration methods such as RTM.

$D(z_0, z_0)$ can be regarded as a virtual source and can be thus propagated down into the earth to generate first-order multiples or higher-order multiples $M(z_0, z_0)$. Compared with equation 1, we can then obtain multiples

$$M(z_0, z_0) = -XD(z_0, z_0), \qquad (2)$$

where X is the response matrix of the subsurface for a reflecting surface; it contains all primary reflections and multiples of the subsurface. The source and the data in equation 1 are replaced with $D(z_0, z_0)$ and $M(z_0, z_0)$ in equation 2, respectively. Equation 2 shows that field data can be considered as a virtual source being excited to illuminate the subsurface and generate multiples. The derivation of equation 2 is fully described in Appendix A. Seismic data containing multiples and primaries can then be considered as a source on the surface that transmits into the earth to generate surface-related multiples. Reflected waves (primaries) generate thefirst-order multiples, while multiples generate higher-order multiples.

Our proposed approach migrates the last upward reflection bounce of the multiples. As shown in Figure 1, the first-order multiple recorded at Mg can be extrapolated backward in time, and cross correlates at X2 with the wavefield that is forward extrapolated with the primary reflection recorded at P. The second-order multiple recorded at Mr can then be extrapolated backward in time, and crosscorrelates with the forward extrapolated first-order multiple recorded at Mg to image the reflector at X3. Each multiple can be imaged by crosscorrelating with another multiple which is one-order higher or one-order lower, or with the primary in the same manner.

RTM of multiples can be implemented by the following steps: forward extrapolation with the recorded data containing both primaries and multiples on the surface, reverse modeling with the predicted multiples on the surface in a shot gather, and cross correlating the above two wavefields at each image point.

Imaging condition for RTM of multiples

There are many migration approaches that can be used to produce an image of the subsurface by extrapolating both the source and the receiver wavefields into the earth (Whitmore, 1983; Chang and McMechan, 1987). RTM, because of its full wave-equation modeling, is a powerful tool to effectively handle multiarrival seismic waves and accurately image overhanging reflectors and steep dips. The imaging condition of RTM consists of crosscorrelating two wavefields, i.e., one from the source and the other from the receivers at each depth level. To use the new information provided by multiples, the reversely extrapolated multiples are crosscorrelated with the forward extrapolated wavefields that contain both primaries and multiples.

The multiple imaging condition can be expressed as a zero-lag crosscorrelation between the source and receiver wavefields:

$$\text{Image}(x,y,z) = \sum_{t=0}^{t\ \max} \{P_F(x,y,z,t) + M_F(x,y,z,t)\} * M_B(x,y,z,t), \quad (3)$$

where image (x,y,z) is the image at location (x,y,z), and $t_{\max}$ is the total recording time. The total data $D(z_0,z_0)$ including primaries $P_F(x,y,z,t)$ and multiples $M_F(x,y,z,t)$ are forward-propagated as the source wavefield, while the receiver multiple wavefield $M_B(x,y,z,t)$ is propagated backward in time.

A surface-related multiple can be reflected more than once at the water surface, so it is composed of various orders of multiples as follows

$$M(x,y,z) = M^1(x,y,z,t) + M^2(x,y,z,t) + M^3(x,y,z,t) + \ldots \quad (4)$$

where $M^1(x,y,z,t)$,$M^2(x,y,z,t)$ and $M^3(x,y,z,t)$ is the first-, the second-, and the third-order multiple, respectively. So equation (3) can be rewritten as:

$$\text{Image}(x,y,z) = \sum_{t=0}^{t\ \max} \begin{bmatrix} P_F(x,y,z,t)+ \\ M_F^1(x,y,z,t)+ \\ M_F^2(x,y,z,t)+ \\ M_F^3(x,y,z,t)+ \\ \ldots \end{bmatrix} * \begin{bmatrix} M_B^1(x,y,z,t)+ \\ M_B^2(x,y,z,t)+ \\ M_B^3(x,y,z,t)+ \\ \ldots \end{bmatrix}. \quad (5)$$

$P_F(x,y,z,t)$,$M_F^i(x,y,z,t)$, and $M_B^j(x,y,z,t)$ will all generate up-going primaries, up-going multiples, down-going primaries, and down-going multiples when they propagate in the media. Expanding equation (5), we obtain equation (6),

$$\text{Image}(x,y,z) = \sum_{t=0}^{t\ \max} \begin{matrix} (P_F(x,y,z,t) * (M_B^1(x,y,z,t) + M_B^2(x,y,z,t) + M_B^3(x,y,z,t) + \ldots))+ \\ (M_F^1(x,y,z,t) * (M_B^1(x,y,z,t) + M_B^2(x,y,z,t) + M_B^3(x,y,z,t) + \ldots))+ \\ (M_F^2(x,y,z,t) * (M_B^1(x,y,z,t) + M_B^2(x,y,z,t) + M_B^3(x,y,z,t) + \ldots))+ \\ (M_F^3(x,y,z,t) * (M_B^1(x,y,z,t) + M_B^2(x,y,z,t) + M_B^3(x,y,z,t) + \ldots))+ \\ \ldots \end{matrix} \quad (6)$$

We then rewrite equation 6 to explicitly express the imaging condition terms:

$$\begin{aligned} \text{Image}(x,y,z) &= \sum_{t=0}^{t\ \max} \begin{bmatrix} P_F(x,y,z,t) * M_B^1(x,y,z,t)+ \\ M_F^1(x,y,z,t) * M_B^2(x,y,z,t)+ \\ M_F^2(x,y,z,t) * M_B^3(x,y,z,t)+ \\ \ldots \end{bmatrix} \\ &+ \sum_{t=0}^{t\ \max} \begin{bmatrix} P_F(x,y,z,t) * M_B^2(x,y,z,t) + \ldots \\ +M_F^1(x,y,z,t) * M_B^3(x,y,z,t) + \ldots \\ +M_F^2(x,y,z,t) * M_B^4(x,y,z,t) + \ldots \\ \ldots \end{bmatrix} \\ &+ \sum_{t=0}^{t\ \max} \begin{bmatrix} M_F^1(x,y,z,t) * M_B^1(x,y,z,t)+ \\ M_F^2(x,y,z,t) * M_B^1(x,y,z,t) + M_F^2(x,y,z,t) * M_B^2(x,y,z,t) \\ M_F^3(x,y,z,t) * M_B^1(x,y,z,t) + M_F^3(x,y,z,t) * M_B^2(x,y,z,t) \\ +M_F^3(x,y,z,t) * M_B^3(x,y,z,t)+ \\ \ldots \end{bmatrix} \end{aligned} \quad (7)$$

In equation 7, the first summation forms an image, the second summation generates migration artifacts, and the third summation does not form an image at all. In line 1 of the first summation, recorded primary reflection energy has reflected again at the free-surface (becoming twice-reflected down-going energy), then propagates forward in time, and then crosscorrelates with backward-propagated three-times-reflected events from receiver locations to form an image. In line 2, recorded three-times-reflected energy has reflected at the free-surface (becoming four-times-reflected down-going energy), then propagates forward, and then crosscorrelates with backward-propagated five-times-reflected events from receiver locations to form an image. In general, recorded (2n − 1)-times reflected events reflect once more at the free-surface to act as down-going virtual source energy that forward propagates and then crosscorrelates with backward-propagated (2n + 1)-times reflected events to form an image. All these summations describe, as does standard migration of single-reflected events, the interaction of forward-propagated source energy with backward-propagated energy that has been caused by a single subsurface reflection of that source energy. In the second summation of equation 7, each term expresses virtual source energy, in the form of down-going 2n-times reflected energy, crosscorrelating with backward-propagated energy that has reflected at least (2n + 3) times. These crosscorrelations produce unwanted crosstalk energy exactly as in standard migration using actual source energy, when the source energy crosscorrelates with multiples (at least three-times-reflected). In equation 7, all the wavefield interactions that are physically possible have been expressed in the first two summations. The third summation contains crosscorrelations that are forbidden from occurring at positive depths by causality. It demonstrates that the first-order multiples forward propagating in time from the source never meet the first-order multiples backward-propagated from the receiver. Generally said, it cannot be constructively imaged when the m-order multiples forward propagate in time and crosscorrelate with the backward-propagated m-or-less order multiples because these events never meet in wavefield propagation.

RTM of multiples needs extrapolating the estimated multiple wavefield backward in time. Thus, multiple attenuation tools can be used to obtain multiples, but do not need to remove the multiples from data set. One of the best of multiple removal approaches is the surface-related multiple elimination (SRME) method developed by Verschuur et al. (1992), and Berkhout and Verschuur (1997). This method is a data-driven multiple attenuation approach that does not need any information of the earth. The surface-related multiple elimination method typically consists of two steps: the first step is prediction of multiples and the second step is subtraction of multiples. In the first step, multiples are predicted by pairwise convolutions of the traces. A first-order multiple can be regarded as two primaries connected at the surface reflection point. It could be possible to combine primary reflections that are already available in the data to construct first-order multiples. Thus, higher-order multiples can be predicted by using multiples that exist in the data. In SRME, the second step is the subtraction. Multiples will be subtracted by estimating the differences between the data and predicted multiples under the L2 norm. The subtraction step is also very challenging for SRME (Spitz, 1999; Luo et al., 2003; Liu, Y. et al., 2009). Fortunately, for RTM of multiples, we can avoid the subtraction step and use the predicted multiples directly. Attenuating multiples is a common data processing process. Here we do not need to attenuate multiples, but instead keep them after data processing. Excluding the calculation time of obtaining multiples, the execution time of RTM of multiples is therefore equivalent to the one of conventional RTM.

NUMERICAL EXPERIMENTS

A three-layer model imaged by multiples

We use a three-layer velocity model with one horizontal and one curved interface shown in Figure 2 to illustrate the migration of multiples. The velocity model is discretized into a 2000 (in X) by 500 (in depth) grid points, with a grid interval of 5 m. There are 200 shots in total, with a shot interval of 25 m. Each shot has 200 receivers, with a receiver interval of 15 m. The total record time is 2.4 s and the sample rate is 2 ms. Sources are in the middle of the spread of receivers, with the first shot position at 2500 m.

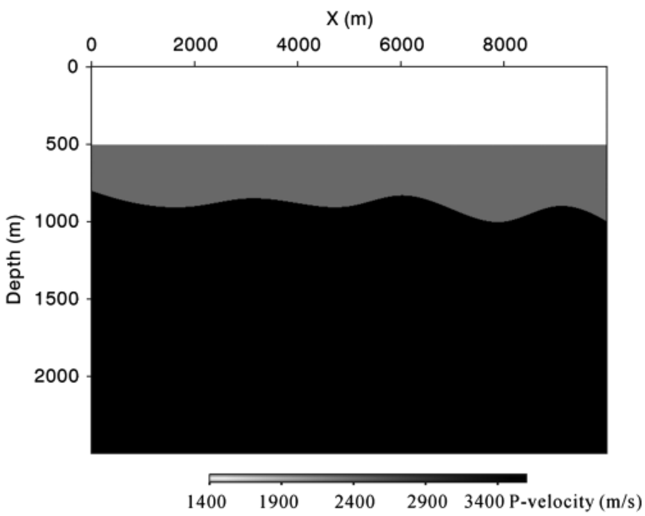

Figure 2. A three-layer velocity model with a flat interface and a deeper curved interface.

Figure 3 illustrates a shot gather that consists of primaries, various order surface-related multiples, and internal multiples. The image after RTM of multiples of this model is shown in Figure 4. This image is generated by using the total data containing both multiple and primary reflections as the source wavefield, and multiples only as the receiver data. C and D are the interfaces of the model that are correctly imaged by RTM of multiples. Other events are artifacts created by various crosstalk events. Event F is the artifact generated by the second-order multiple of the first interface. E is the artifact generated by the second-order multiple of the second interface. G is

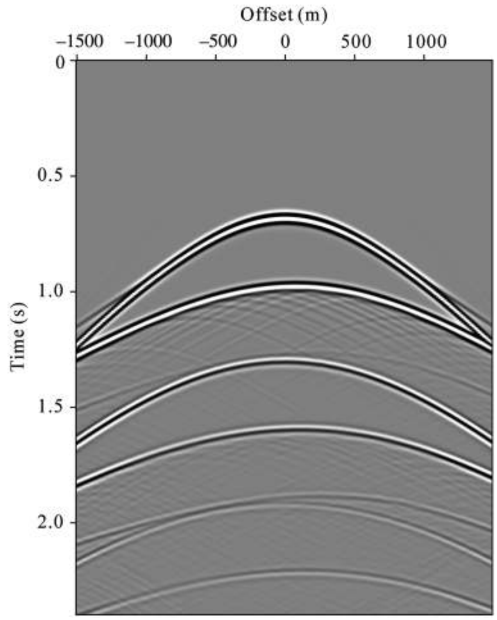

Figure 3. A shot gather with source location at 2500 m from the model in Figure 2 which consists of primaries, various orders of surface-related multiples, and internal multiples.

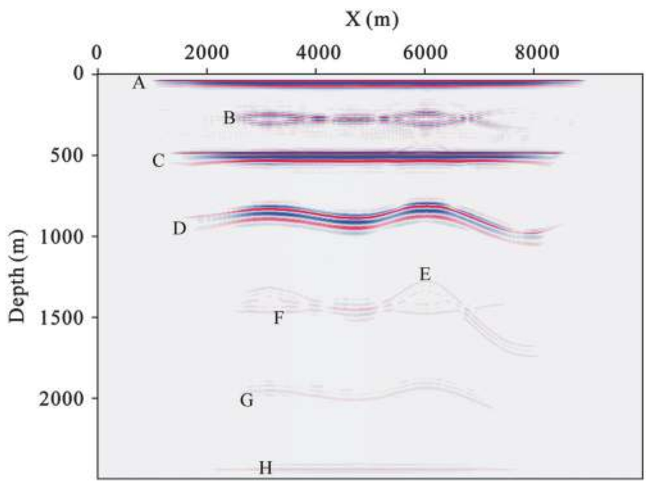

Figure 4. The RTM-of-multiples using multiple and primary reflections as source wavefield and multiple reflections as receiver wavefield. C and D are correctly imaged interfaces. All other events are artifacts created by various crosstalks.

the artifact generated by the third-order multiple of the second interface. B is the artifact generated by the primary of the first interface and the first-order multiple of the second interface. A is the artifact generated by the first-order multiple of the first interface and the second-order multiple of the second interface. The artifacts below the second interface have much weaker amplitudes. The first-order multiples are able to image the interfaces correctly, but higher-order multiples could result in both true and false images.

Sigsbee2B salt imaging by RTM of multiples

The Sigsbee2B (Paffenholz et al., 2002) model contains a sedimentary sequence with a number of normal and thrust faults. The velocity contrast at the water bottom, top, and bottom salt interfaces are able to generate strong free-surface and internal multiples.

The salt body is embedded within a simple sedimentary section ranging from 1437 m/s (4716 ft/s) at mudline to approximately 4511 m/s (14800 ft/s) at a depth of 9144 m (30,000 ft) and containing a number of normal and thrust faults (Figure 5). The salt body's geometry produces significant multipaths and nonhyperbolic moveouts, and results in illumination problems for the conventional migration of primary reflections. The velocity model is composed of a 3201 (in X) by 1201 (in depth) grid points, with grid intervals 7.62 m (25 ft) (in X) and 7.62 m (25 ft) (in depth), respectively. There are 496 shot gathers, with a source interval of 7.62 m (25 ft). For each shot gather, there are 348 traces, with a trace interval of 7.62 m (25 ft). The total time is 12 s and the sample rate is 8 ms. Source depth is the same as the depth of receiver which is 7.62 m (25 ft).

We applied RTM of multiples to the Sigsbee2B data set that contains primaries and multiples. The subsalt image by conventional RTM is shown in Figure 6 and displays poor-illumination problem. The image contains strong specular and nonspecular artifacts created by internal and free-surface multiples and pointed out by arrows. The areas below the overhanging salt and indicated by ellipses are not imaged because of poor-illumination caused by the complex overburden. In conventional data processing, multiples should be attenuated before performing migration, so we applied RTM to the Sigsbee2B data set without free-surface multiples. There are no longer artifacts generated by the free-surface multiples as shown in Figure 7. Vertical dips and overhanging interfaces are now imaged, but the areas below the overhanging salt indicated by the ellipses are still poorly imaged due to weak illuminations. If the acquisition geometry does not provide proper — illuminations, it will be impossible to deliver a complete image of the target, even if the velocity model is accurate. Hence, extra attention is given in recent years to wide-azimuth towed streamer for subsalt imaging. Wide-azimuth acquisition, however, is very expensive and time-consuming.

To obtain an improved subsalt image, RTM of multiples is applied to the Sigsbee2B data. The surface multiple prediction was computed by the SRME method. Below the overhanging salt and indicated by ellipses, where primaries fail to image, multiples

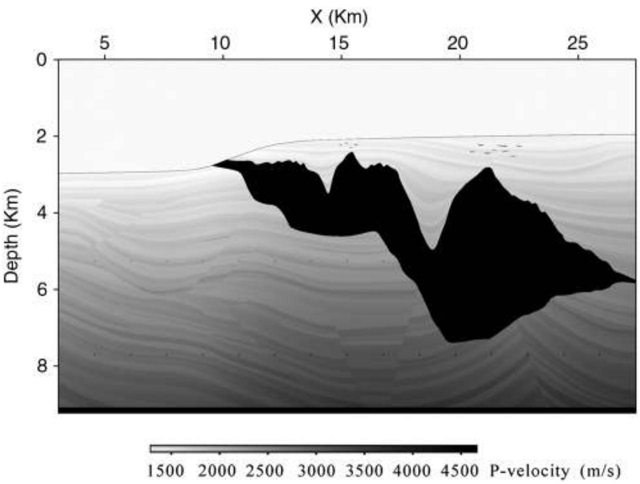

Figure 5. The Sigsbee2B velocity model contains a complex salt body which can result in illumination problems for conventional migration of primaries.

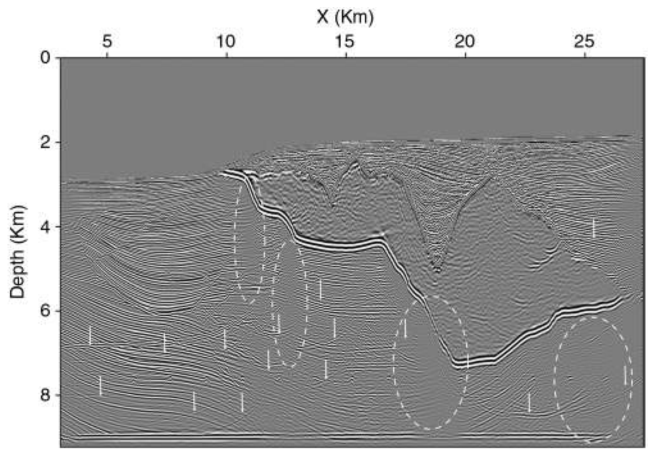

Figure 6. Conventional reverse time migration image without multiple attenuation. It contains strong specular and nonspecular artifacts (indicated by arrows) which are produced by internal and free-surface multiples. The subsalt image indicated by ellipses shows poor S/N due to illumination issues caused by the complex overburden.

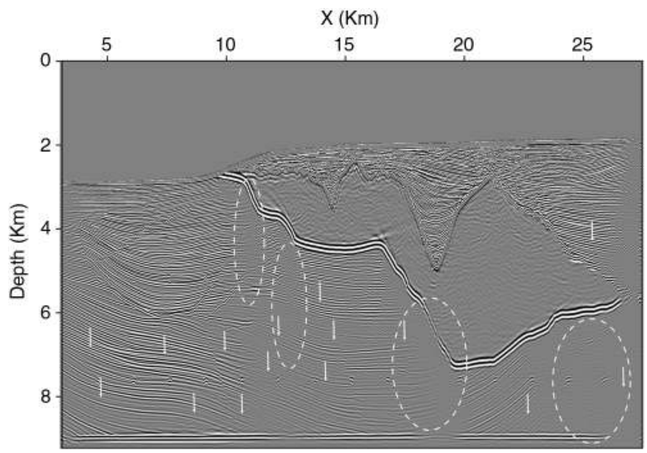

Figure 7. Conventional reverse time migration image after removal of free-surface multiples. It has fewer migration artifacts than Figure 6, but the areas below the salt (indicated by the ellipses) are still poorly imaged due to insufficient illuminations.

produce a robust image. The interfaces and faults are imaged to be continuous, especially in the lower right corner of the model where primaries are not able to image. Although multiples contain a smaller range of reflection angles than primaries, Figure 8 shows that they can be used to provide additional information about subsurface structure. This is caused by the presence of a greater variety of raypaths in the migration of multiples.

To demonstrate the advantages of RTM of multiple, we zoom in the image areas indicated by the ellipses. Figure 9, Figure 10, and Figure 11 are a zoomed view of Figure 6, Figure 7, and 8, respectively. Figure 11 shows that faults and interfaces are much more clearly delineated by the RTM of multiples as compared to Figure 9 and Figure 10, especially in the lower right corner where no dipping faults are imaged due to very poor illuminations in Figure 9 and 10. On one hand, multiples are noises that generate a number of artifact events shown in Figure 9, but on the other hand they offer valuable information to improve the subsalt imaging when they are utilized in migration. In some challenging scenarios, RTM of multiples can lead to great improvement in terms of image quality, and reveals appropriately illuminated seismic features previously impossible to interpret, or in the worse case, simply invisible by conventional migration of primaries.

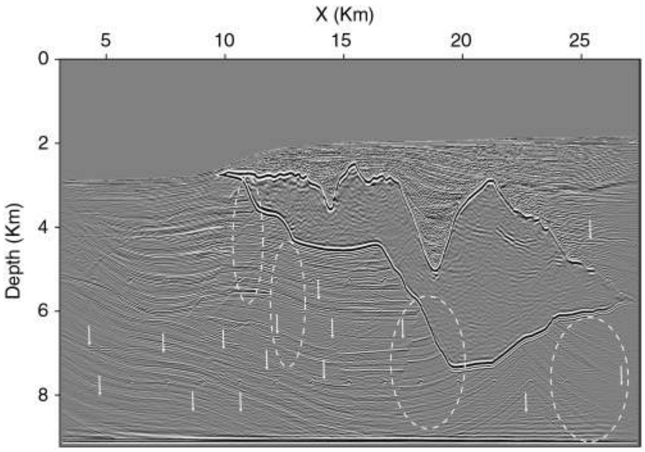

Figure 8. Reverse time migration of multiples. Comparing with Figure 7, the subsalt areas (indicated by the ellipses) are better imaged.

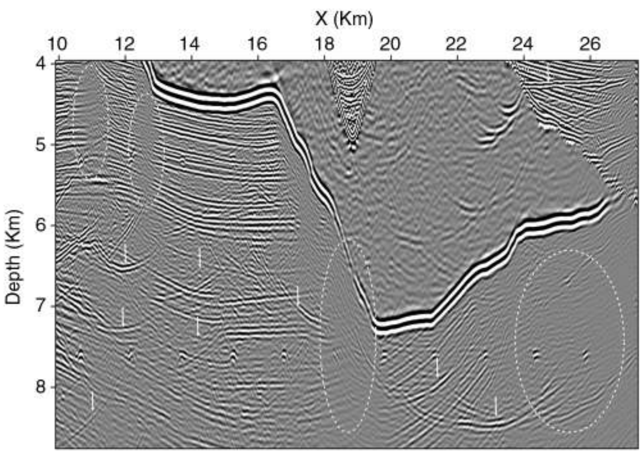

Figure 9. Zoomed view of subsalt images generated by conventional reverse time migration without multiple removal. The arrows point to artifacts and the ellipses represent poor-illumination areas.

DISCUSSION

The Sigsbee2B results are encouraging, but there are still issues that need to be addressed for RTM of multiples. Even though most multiples are migrated to provide valuable information to complement poor illuminations in the subsalt areas where primaries are hard to reach, there still exist crosstalk artifacts generated by migration of multiples (Figure 8). These artificial events result from unwanted crosscorrelation of multiples during the imaging step and are particularly severe when high-velocity contrasts exist. To suppress the imaging artifacts generated by higher-order multiples using the conventional imaging condition, one needs to reduce the nonreflection conditions for various orders of multiples and broaden

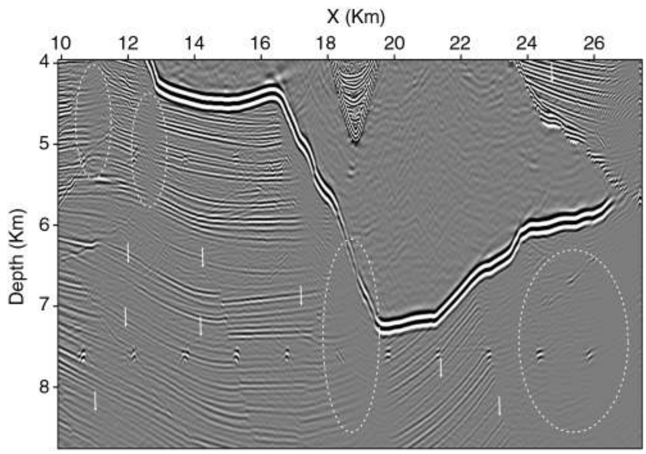

Figure 10. Zoomed view of subsalt image generated by conventional reverse time migration with multiple removal. The arrows point to locations where artifacts in Figure 9 have been removed, whereas the ellipses indicate that the poor-illumination areas still exist.

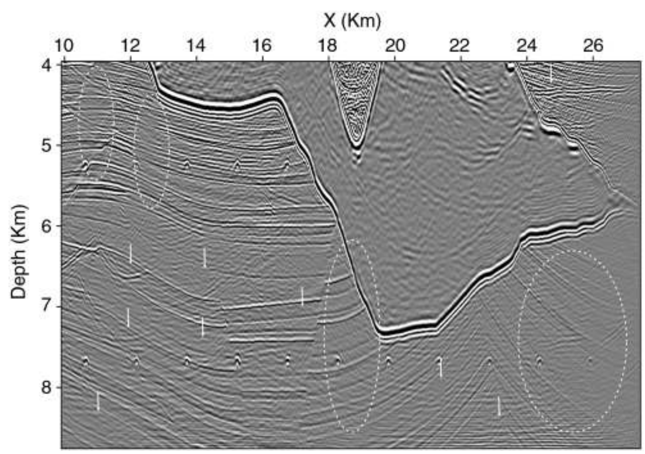

Figure 11. Zoomed view of RTM of multiples image which shows improved subsalt imaging benefited from constructive multiple energy.

the incident angles. A smooth macrovelocity model can be used in conventional RTM, while RTM of multiples might fail as a smooth velocity does not contain interfaces generating multiples.

CONCLUSION

We have proposed a new approach to implement migration of multiples using reverse time migration and apply it for subsalt imaging. The Sigsbee2B test has shown that it is possible to migrate multiple reflections to the correct subsurface location. RTM of multiples can be a powerful tool to provide a wider coverage, a higher fold and a well-balanced illumination of subsalt structures. In the RTM of multiples process, we only need to predict multiples, but do not need to attenuate multiples, which is usually a difficult and challenging task. Precautions need however to be taken because higher-order multiples may crosscorrelate with other higher-order multiples to generate crosstalk migration artifacts.

ACKNOWLEDGMENTS

We thank Gerard T. Schuster and Yi Luo for their helpful suggestions and insightful comments. We are grateful to Isabelle Lecomte, Samuel Gray, Faqi Liu, and Clement Kostov whose constructive comments improved this paper. We would like to thank SMAART JV consortium for offering Sigsbee2B data. The research was funded by the National Nature Science Foundation of China (Grant No. 40930421, 40830422, 40874068) and the National Basic Research Program of China (973 Program, grant No. 2009CB219404).

APPENDIX A

THE RELATIONSHIP BETWEEN MULTIPLES AND SEISMIC DATA

Seismic data recorded at the surface z_0 usually consist of primaries and multiples, which can be presented as follows

$$D = D^{(0)}(z_0, z_0) + M(z_0, z_0), \tag{A1}$$

where, $D^{(0)}(z_0, z_0)$ represents the primary reflections and $M(z_0, z_0)$ represents the multiple reflections. Based on the feedback model of seismic propagation and reflection (Berkhout, 2003), primary reflections can be expressed as

$$D^{(0)}(z_0, z_0) = P(z_0)X(z_0, z_0)S(z_0), \tag{A2}$$

where $S(z_0)$ is a source matrix, $X(z_0, z_0)$ is the response matrix of the earth, and $P(z_0)$ is a geophone response. If the primary is reflected into the earth from the water surface and then back propagates to the water surface again, a surface-related multiple will be generated

$$M(z_0, z_0) = P(z_0)X(z_0, z_0)R(z_0, z_0)D^{-}(z_0, z_0), \tag{A3}$$

where,$D^{-}(z_0, z_0)$ is the up-going wave without geophone effects, and $R(z_0, z_0)$ is the reflectivity at the free-surface. Substituting equation A2 and A3 into equation A1, we can get the primary reflection

$$D = D^{(0)}(z_0, z_0) + P(z_0)X(z_0, z_0)S(z_0)S^{-1}(z_0)R(z_0, z_0) \times P^{-1}(z_0)P(z_0)D^{-}(z_0, z_0). \tag{A4}$$

Comparing with equation A2 and setting

$$A(z_0, z_0) = S^{-1}(z_0)R(z_0, z_0)P^{-1}(z_0), \tag{A5}$$

we get

$$D = D^{(0)}(z_0, z_0) + D^{(0)}(z_0, z_0)A(z_0, z_0)D(z_0, z_0) = D^{0}(z_0, z_0)[I + A(z_0, z_0)D(z_0, z_0)]. \tag{A6}$$

Transforming equation A6, a primary becomes

$$D^{0}(z_0, z_0) = [I + A(z_0, z_0)D(z_0, z_0)]^{-1}D(z_0, z_0). \tag{A7}$$

Equation A7 contains an inverse matrix that is not easy to solve. We change it to a Neumann series to avoid finding the solution directly from the inverse matrix.

$$D^{0}(z_0, z_0) = [I + A(z_0, z_0)D(z_0, z_0)]^{-1}D(z_0, z_0) = D(z_0, z_0) - \sum_{n=1}^{\infty}(-1)^{n-1} [D(z_0, z_0)A(z_0, z_0)]^{n}D(z_0, z_0). \tag{A8}$$

The second term of equation A8 is a predicted multiple,

$$M(z_0, z_0) = \sum_{n=1}^{\infty}(-1)^{n-1}[D(z_0, z_0)A(z_0, z_0)]^{n}D(z_0, z_0). \tag{A9}$$

Setting

$$X = -\sum_{n=1}^{\infty}(-1)^{n-1}[D(z_0, z_0)A(z_0, z_0)]^{n}, \tag{A10}$$

equation A9 can be rewritten as

$$M(z_0, z_0) = -XD(z_0, z_0), \tag{A11}$$

where M represents a predicted multiple, and X represents the response matrix of the subsurface for a reflecting surface, i.e., it contains all primary reflections and multiples of the subsurface. Equation A11 shows that the predicted-multiples can be explained in terms of matrix multiplication of the total data D with the multiple impulse response X.

Equation A11 states that in reverse time migration of multiples, the source is replaced with data $D(z_0, z_0)$. When the data are primary reflection events, they can be forward-propagated in time and crosscorrelated with backward-propagated first-order multiples from the receiver locations to form an image. When the data are multiples, they can be forward-propagated in time and crosscorrelated with backward-propagated higher-order multiples from the receiver locations to form an image.

REFERENCES

Baysal, E., D. D. Kosloff, and W. C. J. Sherwood, 1983, Reverse time migration: Geophysics, **48**, 1514–1524.

Berkhout, A. J., and D. J. Verschuur, 1994, Multiple technology: Part 2, migration of multiple reflections: 64th Annual International Meeting, SEG, Expanded Abstracts, 1497–1500.

Berkhout, A. J., and D. J. Verschuur, 1997, Estimation of multiple scattering by iterative inversion, Part 1 Theoretical consideration: Geophysics, **62**, 1586–1595.

Berkhout, A. J., and D. J. Verschuur, 2003, Transformation of multiples into primary reflections: 73rd Annual International Meeting, SEG, Expanded Abstracts, 1925–1928.

Brown, M. P., and A. Guitton, 2005, Least-squares joint imaging of multiples and primaries: Geophysics, **70**, no. 5, S79–S89.

Chang, W. F., and G. A. McMechan, 1987, Elastic reverse-time migration: Geophysics, **52**, 1365–1375.

Claerbout, J. F., 1968, Synthesis of a layered medium form its acoustic transmission response: Geophysics, **33**, 264–269.

Glogovsky, V., E. Landa, and J. Paffenholz, 2002, Integrated approach to subsalt depth imaging: Synthetic case study: The Leading Edge, **21**, 1217–1223.

Guitton, A., 2002, Shot-profile migration of multiple reflections: 72nd Annual International Meeting, SEG, Expanded Abstracts, 1296–1299.

He, R., B. Hornby, and G. Schuster, 2007, 3D wave-equation interferometric migration of VSP free-surface multiples: Geophysics, **72**, no. 5, 195–203.

He, R., and G. Schuster, 2003, Least-squares migration of both primaries and multiples: 73rd Annual International Meeting, SEG, Expanded Abstracts, 1035–1038.

Huang, T., Y. Zhang, H. Zhang, and J. Young, 2009, Subsalt imaging using TTI reverse time migration: The Leading Edge, **28**, 448–452.

Jiang, Z., J. Sheng, J. Yu, and G. T. Schuster, 2007, Migration methods for imaging different-order multiples: Geophysical Prospecting, **55**, 1–19.

Kessinger, W., and M. Ramaswamy, 1996, Subsalt imaging using mode converted energy and acoustic depth migration: 66th Annual International Meeting, SEG, Expanded Abstracts, 566–569.

Liu, F., G. Zhang, S. A. Morton, and J. P. Leveille, 2009, An optimized wave equation for seismic modeling and reverse time migration: Geophysics, **74**, no. 6, WCA153–WCA158.

Liu, Y., D. Jin, X. Chang, and H. Sun, 2009, Multiple subtraction using statistically estimated inverse wavelets: 79th Annual International meeting, SEG, Expanded Abstracts, 3098–3102.

Luo, Y., P. G. Kelamis, and Y. Wang, 2003, Simultaneous inversion of multiples and primaries: Inversion versus subtraction: The Leading Edge, **22**, 814–818.

Muijs, R., J. O. A. Robertsson, and K. Holliger, 2007, Prestack depth migration of primary and surface-related multiple reflections: Part I — Imaging: Geophysics, **72**, no. 2, S59–S69.

O'Brien, M. J., and S. H. Gray, 1996, Can we image beneath salt?: The Leading Edge, **15**, 17–22.

Paffenholz, J., B. Mclain, J. Zaske, and P. J. Keliher, 2002, Subsalt multiple attenuation and imaging: observations from the Sigsbee2B synthetic data set, 72nd Annual International Meeting, SEG, Expanded Abstract, 2122–2125.

Reiter, E. C., M. N. Toksoz, T. H. Keho, and G. M. Purdy, 1991, Imaging with deep-water multiples: Geophysics, **56**, 1081–1086.

Rosenberg, M. V., 2000, How much does salt obstruct the subsalt image?, 70th Annual International Meeting, SEG, Expanded Abstracts, 582–585.

Schuster, G. T., J. Yu, J. Sheng, and J. Rickett, 2004, Interferometric/daylight seismic imaging: Geophysical Journal International, **157**, 838–852.

Shan, G., 2003, Source-receiver migration of multiple reflections: 73rd Annual International Meeting, SEG, Expanded Abstracts, 1008–1011.

Sheng, J., 2001, Migration of multiples and primaries in CDP data by crosscorrelogram migration: 71st Annual International Meeting, SEG, Expanded Abstracts, 1297–1300.

Spitz, S., 1999, Pattern recognition, spatial predictability, and subtraction of multiple events: The Leading Edge, **18**, 55–58.

Vasconcelos, I., R. Snieder, and B. Hornby, 2008, Imaging internal multiples from subsalt VSP data — Examples of target-oriented interferometry: Geophysics, **73**, no. 4, S157–S168.

Verschuur, D. J., and A. J. Berkhout, 2005, Transforming multiples into primaries: experience with field data: 75th Annual International Meeting, SEG, Expanded Abstracts, 2103–2106.

Verschuur, D. J., A. J. Berkhout, and C. P. A. Wapenaar, 1992, Adaptive surface-related multiple elimination: Geophysics, **57**, 1166–1177.

Whitmore, N.D.Iterative depth migration by backward time propagation: 53rd Annual International Meeting, SEG, Expanded Abstracts, 382

Yu, J., and G. Schuster, 2002, Joint migration of primary and multiple reflections in RVSP data: 72nd Annual International Meeting, SEG, Expanded Abstracts, 2373–2376.